Applied Mathematics & Information Sciences
An International Journal

http://dx.doi.org/10.18576/amis/190510

Skin Cancer and Benign Lesion Classification Using Machine Learning Algorithms

Saleh Ali Alomari

Faculty of Information Technology, Jadara University, 21110 Irbid, Jordan

Received: 12 Mar. 2025, Revised: 12 May 2025, Accepted: 20 Jun. 2025
Published online: 1 Sep. 2025

Abstract: In recent years, skin cancer proved to be one of the fatal types of cancer, which include basal carcinoma, squamous cell carcinoma, and melanoma. Early detection of skin cancer is highly important for efficient cure of this disease. Interest in automatic techniques for image analysis has been growing among the medical and computer research communities in an effort to provide early, reliable information on nature and types of lesions. In this respect, computer vision can play vital role in diagnosis of diseases using non-invasive methods such as medical imaging and images. This paper proposes a new system for detection of skin cancer and benign lesions in medical images using machine learning algorithms. In this system, detection progresses through four main steps: establishment of database of dermoscopy images, image pre-processing, image segmentation using thresholding, and feature filtering and statistical feature extraction via the Gray Level Co-occurrence Matrix (GLCM) and Asymmetry, Border, Color, and Diameter (ABCD) analysis. The proposed system was applied on dataset of 5,500 dermoscopy images and the features extracted by this system were classified into cancer lesions and normal lesions by using three classification methods: the k-nearest neighbor (*K*NN) algorithm, support vector machine (SVM), and nave bias (NB) classifier. The experimental results uncovered that the highest overall accuracy of skin lesion detection and diagnosis (94.35%) was produced by the SVM classifier.

Keywords: Skin Cancer; Computer Vision; Machine Learning; *K*NN Algorithm; SVM; NB Classifier; Dermoscopy Images.

1 Introduction

Technology, in general, and artificial intelligence, in particular, are ever developing and penetrating almost every aspect of modern life. Medicine is among the fields benefitting from developments in technology the most, especially in early detection and diagnosis of fatal diseases like cancer, which allows for successful treatment of disease and better healthcare outcomes. Evidence supports that cancer is currently a major cause of death worldwide. It has proved to be one of the most serious common diseases. For example, about 1,958,310 people have been diagnosed with cancer in 2023. Currently, this disease is regarded as one of the leading public health challenges in the World. The number of deaths because of cancer was estimated worldwide by applying the data-driven join point algorithm. The estimates revealed that this disease is the second largest cause of mortality before the age of 70 in more than half of the countries in the World. The statistics and estimates indicate that it is more fatal than the Acquired Immunity Deficiency Syndrome (AIDS), tuberculosis, and malaria combined. Furthermore, it was estimated that this disease will cause the death of more than 10 million people annually around the World [1].

For a better understanding of skin cancer, it is important to realize what usually happens when a healthy cell turns into a cancer cell. It is possible for a cancer cell to develop anywhere in the body. Usually, this happens when cells grow out of control, making it difficult for the body to deal with them properly. The body consists of several types of cells. In the normal condition, these cells grow, divide to produce new cells, and die when the body is in need for this and they do not spread away from their place of origin in the body. This sequential process helps the body to stay safe and healthy, but, at times, some of those cells divide when there is no real need for any new cells, thus crowding the normal cells. These extra cells generate mass of tissues called tumor, which can either be malignant or benign [2].

Benign tumors can be removed without harm or side effects, and, in most of the cases, they do not return back again. Moreover, they do not spread to other parts of the

* Corresponding author e-mail: omari08@jadfara.edu.jo

body, and, most importantly, they pose no risk to the human life. The malignant tumors, to the contrary, are cancer itself. The cells in these tumors are abnormal because they divide without control and they have the ability to penetrate and damage the tissues and organs adjacent to them. In addition, the cancer cell can separate from the malignant tumor and enter the blood stream and the lymphatic system. It can spread from its original location to other locations and form other tumors in different organs in the body. This process is called metastases [3].

Cancer has many types that are commonly categorized based on the location of cancer cell emergence or development. It can start in the lungs, breasts, bones, skin, colon, or even the blood. So, the different types of cancer are usually differentiated from one the other, and named, according to the location where each one develops. Though the different kinds of cancer are similar in some traits, they differ in the ways how they grow and spread. For example, the cancerous cells in the lung can spread to the bone and grow there. When the lung cancer cells spread to the bones, the cancer is still described as lung cancer. Even though the cancer cells in the bones are very similar to the cancer cells in the lung, the cancer in the bones will not be called bone cancer unless it originated in the bone [4].

The three most common types of skin cancer are (i) the Basal Cell Carcinoma (BCC); which is ranked as the first global cancer disease in terms of spread; (ii) Squamous Cell Carcinoma (SCC); and (ii) Melanoma. Besides these, there are rare types of skin cancer like those that originate in the sweat glands [2]. Although skin cancer often appears in late ages (e.g., older adults), skin damage begins at an early stage due to exposure to ultraviolet (UV) light, especially during sunburning. Thereupon, the best way for preventing skin cancer is protecting the skin from the UV rays by, mainly, avoiding, or reducing, direct exposure to the Sun. This can be achieved when one knows the UV Index, which is an index that shows the intensity of sunlight [2]. One can also check herself/himself, at any time, by checking indicative signs on her/his body such as the appearance of new spots that differ from other spots in the surrounding skin parts like sore that does not heal or moles or freckles that changed in size, shape, and/or color. However, many tests are in use nowadays for the detection and diagnosis of cancer. But satisfactory diagnosis is performed by examination of biopsy sample of the suspected cancerous tissue.

Cancer can be caused by various factors. However, its exact causes are still largely unknown. Scientists can determine the possibility of cancer in the body based on factors that increase the risk for cancer such as tobacco smoking, pollution, radiation exposure, asbestos ingestion, genetic predisposition, and long-term exposure to sunlight, which are causal factors for skin cancer. Furthermore, long-term exposure to UV radiation or even to the light that is used to change skin color in beauty centers and eating unhealthy foods can cause cancer [5].

Cancer treatment is very complex. It usually, requires participation of diverse groups of healthcare professionals, including physicians of all disciplines like family physicians, surgeons, oncologists, pathologists, radiologists, physiotherapists, and, even, general practitioners [6]. Cancer development is categorized into stages (e.g., the first stage) that reflect the extent of its spread in the body and its seriousness. The cancer stage is specified based on the results of biopsy analysis, which help in determining the type of cancer and extent of its spread in the body. Staging helps the caregivers to determine the most appropriate treatment protocols. Generally, the cancer stage is described numerically by assigning a number to it that ranges from 0 to 4. The higher the stage of cancer, the more aggressive and widespread in the body the cancer is [2].

2 Theoretical Background

Skin constitutes the largest part of the human body; it accounts for about 15% of the total adult body weight. It acts as barrier that protects the body from injury and it controls the body temperature and prevents any loss of the body fluids. It consists of two major layers; the dermis and epidermis, which are underlain by layer of fatty tissues [7]. Therefore, skin cancer can be simply defined as the uncontrolled growth of abnormal cells in the skin. These cells can grow into a tumor, which can either be benign or malignant. A malignant tumor in the skin indicates the onset of skin cancer, which can arise in every host cell in the skin. The main cause of this type of cancer is extended exposure to UV radiation, which is regarded as carcinogen owing to that it affects every carcinogenesis stage [10]. Afterwards, the skin cancer cells may spread to other parts of the body and generate tumors in them.

So far, there are 200 known types of skin cancer, the most common of which is BCC, which is one of the most popular cancer types in the United States. It usually starts in the lower layer of epidermis and rarely spreads to the remainder of body or leads to death. However, it is still serious as it can invade the surrounding tissues, causing destruction and deformation. It accounts for about 70% of the skin cancers. The second most popular type of skin cancer is SCC. It is often found on body areas that are damaged by UV radiation from the Sun or the tanning beds. The areas affected by it are parts of the skin that are exposed for prolonged time to the Sun rays, which encircle the neck, head, chest, ears, upper back, arms, lips, hands, and legs. It usually develops in the epidermis upper layer and constitutes alone nearly 30% of all skin cancer types [7]. Melanoma, the third popular cancer type, emanates in the skin melanocyte cells. Albeit it is not as common as the SCC and BCC, it is regarded as the most serious skin cancer type owing to that it is more

probable to spread to other body parts like the lungs, lymph nodes, brain, bones, and liver, than the other skin cancer types, particularly when it is not detected early.

Skin cancer is a serious contemporary disease that is difficult to detect in the early stages. It is attracting attention of researchers and physicians and it has become a problem of great concern to everyone the individual level because of its substantial threat to the human life since at least 40% of people with white skin are likely to be exposed to it. Besides, people with low immunity as a result of taking drugs that weaken the immune system and people with the Human Immunodeficiency Virus (HIV), i.e., people suffering from the AIDS, are almost equally likely to have this type of cancer [7].

For efficient treatment of skin cancer, the physicians and other healthcare professionals need to know the exact type of skin cancer involved. Most skin cancers start in the top layer of the skin, i.e., the epidermis. The most prevalent skin cancer types are SCC and BCC. However, non-melanoma skin cancer (NMSC) is one of the most frequently diagnosed types of cancer. Early detection of cancer is of paramount importance. Quite often, the skin cancer is identified based on cell growth, behavior, and metastatic ability. Of all skin cancer types, the SCC and BCC have good prognosis, particularly when they are detected at their early stages [10].

The researchers in [8] proposed a method for skin cancer detection using image processing. The paper [8] describes how they used various methods and algorithms to analyze images and presents the analysis results. One of those methods was the Convolutional Neural Network (CNN), which was employed to enhance image quality, and the ANN with the back propagation training algorithm for classification.

In [9], the researchers proposed detection of skin cancer by deep learning and sound analysis algorithms. They employed CNN based on the Inception V2 network, in which the dermoscopic images were validated by biopsy reports, which classified the tissues as either benign or malignant. These researchers utilized publicly-available datasets like the International Skin Imaging Collaboration (ISIC) dataset, which consists of 4,361 images. They employed the k-means clustering algorithm in order to cluster activations into distinct groups of related observations.

Skin cancer is one of the most common diseases. Millions of people die because of it, especially in the United States. Statistics show that 1 in every 5 Americans will be exposed to skin cancer in her/his lifetime. The major cause of this cancer is prolonged exposure to the UV radiation in the sunlight, which causes various skin or epidermis layer diseases. This radiation is categorized into two types, ultraviolet A (UVA) radiation, which passes deep into the skin, and ultraviolet B (UVB) radiation, which is more likely than UVA radiation to cause sunburn to the skin. It should be recalled, however, that not only sunlight rays that can cause skin cancer but also the artificial rays that are used in tanning and laser treatments [11].

The epidermis is metabolically-active tissue that is located in the outermost layer of the skin, which has no capillaries or veins. Its thickness is around 0.2 mm on the average. It varies based on location on the body. As Fig. 1 shows, the human skin consists of three layers of epidermis that are divided into five sublayers, which are stratum basale, stratum spinosum, stratum granulosum, stratum lucidum, and stratum corneum. Dermis is the second skin layer. It lies below the epidermal layer. It is much thicker than the epidermis (often 1–4 mm). Its main components are elastin and collagen fibers. There are much more fibers and much fewer cells in the dermis than in the epidermis. The subcutis, also known as the hypodermis in histology, is the third layer. It lies right below the dermis. It is elastic layer that includes large number of fat cells that function as shock absorbers for the blood vessels and the nerve endings. Thickness of this layer ranges from 4 to 9 mm on the average. It differs from one person to another and depends on the part of the body it overlays [12, 13].

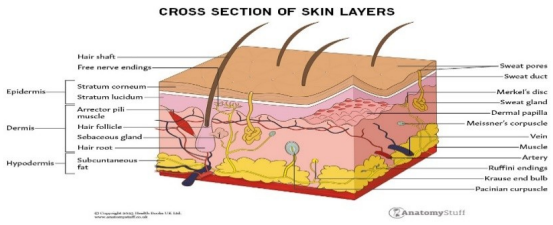

Fig. 1: Human skin layers and sublayers.

2.1 Squamous Cell Carcinoma (SCC)

There are three main types of skin cancer, one of which is SCC. It is the second most common type of skin cancer in the UK. Usually, it is caused by long exposure to UV light from the Sun or sunbeds, which cause particular cells, namely, the keratinocytes, in the outer skin layer (i.e., epidermis), to grow out of control into tumor. This can take place on any body part, but it most often occurs on areas exposed to the Sun, that is, the neck; head, including the ears; lips; and backs of the hands. As well, the SCC can develop where the skin has been damaged by ulcers, X-rays, and burns and on persistent chronic wounds and old scars. It affects old people mainly, even the ones who tend to avoid the Sun. In addition to the old people, it affects the farmers, builders, sailors, and surfers; the people who are often out in the Sun. People with fair skin are more at risk of developing SCC than people with dark skin. Anyone who experienced extended UV light treatment for skin conditions like psoriasis will

too be at an increased risk of developing SCC. This cancer type can vary greatly in appearance, but most SCC appears as crusty or scaly lump or skin, with red, inflamed base that is not painful [15, 19].

2.2 Basal Cell Carcinoma (BCC)

The BCC usually develops in the lower part of the epidermis, which is called the basal cell layer. In this cancer type, the basal cells constantly divide to form new cells to replace the squamous cells that wear off the surface of the skin. It is the most common type of skin cancer, accounting for more than 80% of all skin cancer cases in the UK. As these cells move up in the epidermis, they get flatter, eventually becoming squamous cells. The main cause of this sort of cancer is high exposure to UV light from the Sun or from sunbeds. It may develop anywhere on ones body, but it is most common on those areas that are frequently exposed to the Sun, namely, the head, face, ears, and neck. It may also develop where ulcers, scars, or burns have damaged the skin. However, it mainly affects the fair-skinned adults. People having other types of skin too are at risk, including people with a pale skin that burns easily; people with red or light-colored hair who do rarely tan, albeit some may have dark hair but still have fair skin; and those who had lengthy exposure to the Sun like the outdoor workers, the people having outdoor hobbies, the people who live in sunny climates, and the people who sunbathe or use sunbeds.

2.3 Melanocytes

These cells form the brown pigment melanin, which gives skin its brown or tan color. This pigment acts as natural sunscreen of the body that protects the deeper skin layers from some of the harmful impacts of the Sun. The melanoma skin cancer usually begins in these cells [19]. Fig. 2 shows the locations of the three most common types of cancer in the skin.

Neuroendocrine Carcinoma Neuroendocrine carcinoma is a kind of skin cancer that develops in neuroendocrine cells, which are cells that produce hormones in response to nerve impulses. Skin cancer, unlike moles, has the ability to infect adjacent normal tissues and spread throughout the body [20].

3 Related Applications

Skin cancer became a serious disease that threatens survival and quality of life of millions of individuals worldwide. To better deal with it, the healthcare professionals need to detect it as early as possible; before

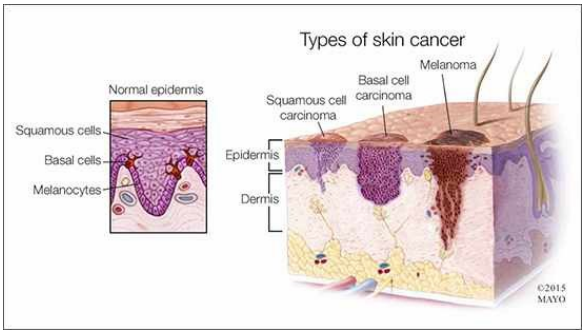

Fig. 2: Locations of the three most common types of cancer in the skin [11].

it spreads in the body, through advanced techniques and modern technology that allow for easier, faster, and more efficient detection of it than traditional techniques and methods. In [21], the researchers proposed detection of melanoma skin cancer by using image processing and machine learning. The model they proposed was designed in three phases, each of which had specific purpose to serve. The first phase was creation of dataset of images that had been obtained from the dataset of ISIC and pre-processing of images by removing hair, glare, and shading using MATLAB. Removal of these image features helps in identification of tumor color, texture, shape, and size in efficient manner. The second phase consisted of image segmentation and feature extraction. Segmentation was carried out by three methods: (i) Otsu segmentation method, (ii) the modified Otsu segmentation method, and (iii) the watershed segmentation method. On the other hand, the features were categorized based on shape, color, texture, and size. The third phase was designing a skin cancer detection model and training it. The model these researchers proposed was trained on the dataset that had been compiled in Phase 1 using the Artificial Neural Network (ANN) with the back propagation algorithm, the Support Vector Machine (SVM), and CNN. After its training, the model was tested for accuracy.

The researchers in [19] suggested skin cancer detection using image processing and the SVM classifier. The Gray Level Co-occurrence Matrix (GLCM) was employed for extraction of features from the images that can be useful for classification [19]. A classifier was, then, employed to identify cancerous cells in the images and differentiate them from other diseased and healthy cells. For simplicity, the SVM classifier was employed. This classifier takes a set of the images and for each individual one of them it predicts to which of two categories (non-cancerous or cancerous cells) the particular cells belong. The purpose of the SVM is to create a hyperplane that separates the two classes under consideration with maximum separation. The outputs of the GLCM are used as input to the SVM classifier which

employs training data, testing data, and grouping information to decide on whether the cells in the given input image are non-cancerous or cancerous [22].

In [23], the researchers developed a system for melanoma diagnosis that is a combination of segmentation method and analytical method. It aimed at improving these two methods and developing interface that can help the dermatologists in melanoma diagnosis. A number of preprocessing steps were followed in order to remove the noise and any unwanted features from the image. Then, an automatic segmentation approach was employed to locate the skin lesion. The next step was extraction of features followed by implementation of the Asymmetry, Border, Color, and Diameter (ABCD) rule for diagnosis through calculation of the Total Dermatoscopic Value (TDV) score. Diagnosis targeted three kinds of skin lesions: melanoma, suspicious lesions, and benign lesions. Experiments were conducted on 40 images with suspicious melanoma.

(Fig. 3) describes melanoma detection of lesions according to this method, in which image preprocessing is highly important step in lesion diagnosis. It is applied to correct for any defects in illumination, eliminate the noise and small spots, and improve the overall image quality. For classification of the skin lesions and distinction of melanoma from benign lesions, segmentation must begin by isolating the lesion from the healthy skin in the color image by using suitable segmentation method which must be accurate well enough for this purpose. Afterwards, the image is subjected to post processing so as to remove the pixels isolated by segmentation in the area of the lesion. The ABCD feature extraction method is a method that can provide objective and reproducible diagnosis of the skin cancers. In addition, it has good speed of calculation. It is based on four parameters: Asymmetry (A), which relates to assessment of lesion asymmetry; Border (B), which estimates border of lesion; Color (C), which determines the number of the colors that exist in the lesion; and Diameter (D), which expresses lesion diameter. After values of the four aforementioned lesion characteristics have been obtained, classification is implemented [23].

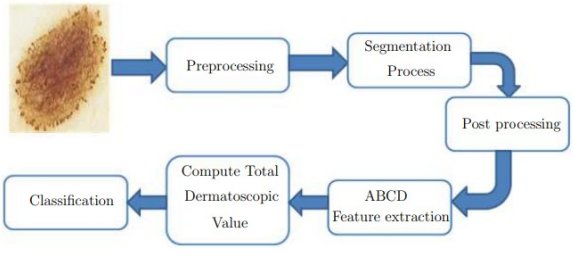

Fig. 3: Architecture of System for Melanoma Skin Cancer Diagnosis [23].

A method for detection of cells with skin cancer using image processing is presented in [24]. The method consists of four fundamental processes: image preprocessing, image segmentation, feature extraction, and classification. Image preprocessing includes hair removal by using Dull-Razor, noise removal, image sharpening, and image resizing. Meanwhile, image segmentation is used to segment the region(s) of interest in the image. The segmentation algorithms commonly employed encompass the k-means and the histogram thresholding algorithms. As to classification, various algorithms can be employed. The recent skin cancer detection methods use algorithms that are based on machine learning and deep learning for classification. The classification algorithms most commonly employed are the SVM, feed-forward ANN, and deep CNN.

Computer-aided diagnosis of disease helps the physicians and dermatologists in obtaining second opinion for appropriate analysis and treatment of the skin cancer. An Automatic Lesion Detection System (ALDS) for skin cancer classification that uses SVM and neural classifiers was developed by [25]. These researchers focused on development of an improved ALDS framework based on the probabilistic approach that utilizes the active contours and watershed-merged mask for segmentation of the mole. Later to that, the SVM and neural classifier are employed for classification of the segmented moles.

Reliable, early detection of skin cancer is a major problem in medicine. In this regard, artificial intelligence and advanced technology are tools that can enable easy, early detection of this disease. Table 1 presents comparison between a number of previous, relating studies, with particular emphasis on accuracy of tumor classification.

4 Overall System

Detecting the skin cancer early enough before it spreads out in the body can help the physicians better treat it. This paper proposes a new method for skin cancer detection and describes it. The method consists of several steps. The paper also demonstrates how the patient herself/himself can inspect any suspicious areas on the body so that she/he can know whether the spots in the suspicious areas correspond to benign or malignant tumor.

Fig. 4 depicts the proposed system and illustrates how it works. It spotlights all operations of the system that work in tandem to perform the due task and deliver the final classification result following specific rule.

Table 1: Comparison between Previous Studies Proposing Skin Cancer Detection Methods

Researcher(s)	Merit	Dataset(s) and Number of Images	Accuracy
Vijayalakshmi [21]	Support Vector Machine (SVM) and Non-Convolutional Neural Network	Dataset of 1000 1500 images from the International Skin Imaging Collaboration (ISIC) database	∼
Bano and Sarode [16]	Better classification accuracy using SVM	Dermoscopic Images	SVM: 95%
Smaoui and Bessassi [17]	Total Dermatoscopic Value (TDV) Method	DermIS and DermQuest, including melanoma and non-melanoma cases	92.5%
Jana, Subban, and Saraswathi [18]	ANN, SVM, and Back Propagation Neural Network (BPNN)	100 images from DermIS, DermQuest, and ISIC datasets	SVM: 74.36%, Polynomial: 85.3%, RBF: 68%
Farooq and Azhar [25]	SVM and ANN for classification	Melanoma and non-melanoma images from DermIS and DermQuest	Overall: 80%

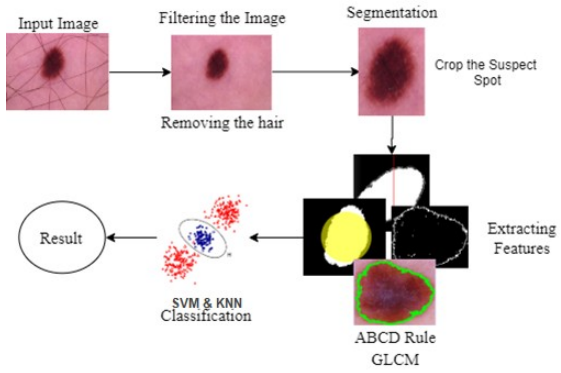

Fig. 4: Description of the Proposed System for Skin Cancer Detection.

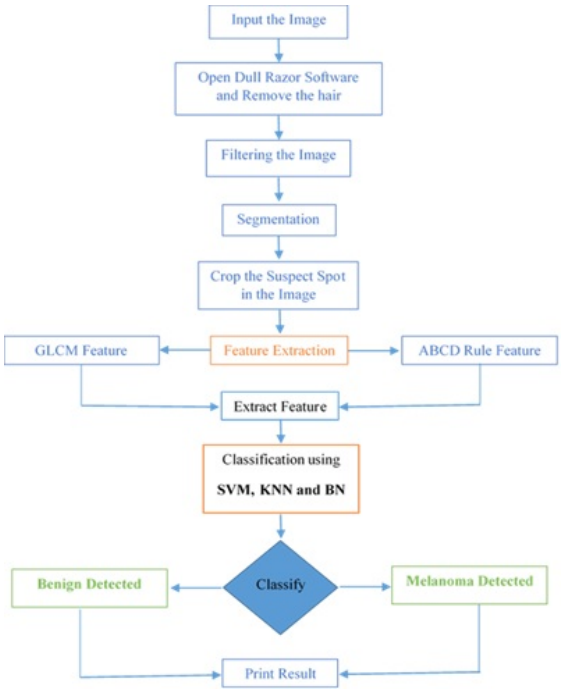

Fig. 5: Flow Diagram of the Steps of the Proposed System for Skin Cancer Detection.

4.1 Proposed System and Design

Any system to be proposed for lesion detection should have high sensitivity, specificity, and accuracy and short time to decide on the type of the skin cell, whether it is cancerous or benign. Moreover, it must be easy to use by the physicians and the other medical staff. Specifications of domains may be articulated by using certain domain definitions or jargon. The domain requirements are important because the basic principles for application domain are usually reflected. The system may not operate successfully if these requirements were not satisfied.

Fig. 5 outlines the steps followed in skin cancer detection according to the system proposed by the researcher in this paper. It highlights the steps and shows their flow sequence.

1. Inputting the Image

An image must be input to the system first. The herein proposed system supports different image formats like the jpg, png, and tif formats. The dataset that was employed in the current study for training, validation, and testing had been downloaded from archive of the ISIC [26]. This archive contains more than 20,000 open source, free access dermoscopy images that were obtained from numerous clinical centers around the World. Over time, this archive was utilized to test and validate a large number of methods proposed for segmentation and classification of skin lesions. Furthermore, it constitutes

public source of images for teaching and development. This archive includes images of both malignant and benign lesions [27].

Fig. 6: Three kinds of images: (i) contextual image, (ii) macro image, and (iii) micro image.

A variety of imaging devices can be used for dermatological imaging and image acquisition like tablet attachments, point-and-shoot cameras, and smartphones. Within this context, three types of images are necessary for accurate diagnosis of skin condition (Fig. 6): macro images, micro images, and contextual images.

2. DullRazor Software

The image is input to DullRazor software to remove hair from it for enhanced clarity and classification outcomes. The output image must have a tif format only.

3. Filtering the Image

Image filtering is the process of removing unwanted information from the image. Filtering the image from impurities after hair removal improves the accuracy of extraction of features from it. In addition, this process removes different sorts of noise from the image [28],[29]. Fast median filtering is one of the filtration methods which we used in this work. The median filter works by going through the signal entry by entry and replacing each entry with the median of neighboring entries. It slides entry by entry across the entire signal. The pattern of neighbors is known as the window. Complex window patterns like the **cross** or **box** patterns with odd numbers of entries are possible in the two-dimensional (2D) images [30]. The middle value after all entries in window have been numerically sorted is shown in Fig. 7.

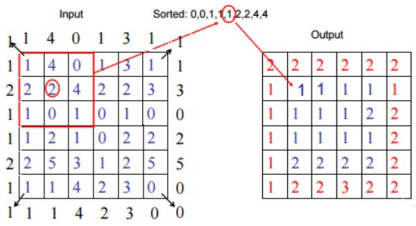

Fig. 7: Example of Two-Dimensional (2D) Median Filtering by Using 3x3 Sampling Window.

4. Segmentation

Image segmentation can be defined as the process of dividing digital image into several homogeneous, non-overlapping, constituent segments. In the segmentation process, the image is divided so as to specify the locations of suspicious areas in it. When the isolated objects of interest are the simplest and easiest to analyze, segmentation should be ended. The thresholding method is the most basic method of image segmentation. To convert a grayscale image to a binary image, this method uses a clip-level (or a threshold value). Balanced histogram thresholding is also available. The most important step in this method is defining the threshold value or values when several levels are chosen. In the industry, various popular methods are employed, including Otsu's method, k-means clustering, and the maximum entropy method [26].

5. Cropping the Suspect Spots in the Image

After identifying the suspicious areas in the image, they are cropped to keep only the suspicious spot(s).

6. Feature Extraction

After cropping the suspicious areas in the images, the cropped image is subjected to feature extraction in an effort to extract all meaningful features from it. Two rules have been employed for this purpose: the ABCD Rule and GLCM. Shape, color, and texture features were extracted from the segmented images after selecting the lesion in the segmentation step. Because these images contain statistical texture features, they were extracted using one of the most popular algorithms; the Local Binary Pattern Features (LBPF) and GLCM algorithms [31]. Besides, the ABCD dermoscopy features are highly important in distinguishing the benign from the cancerous skin lesions. Criteria for identifying ABCD features in the different methods that are employed in diagnosis of skin cancer can be evaluated using information from macroscopic images as shown in Fig. 8. This information relates to

asymmetry, border irregularity, color variation, and diameter. These image characteristics, when combined, provide us with satisfactory distinction between the malignant and benign skin lesions [32], [33], [34].

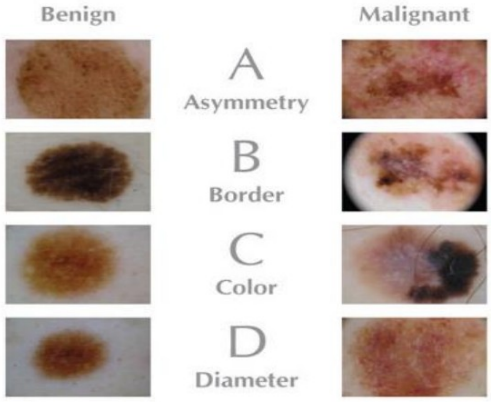

Fig. 8: Dermoscopy Features: (A) Asymmetry, (B) Border Irregularity, (C) Color, and (D) Diameter.

7. The ABCD Rule Features

In feature extraction using the ABCD rule, four image characteristics are analyzed: asymmetry, border, color, and diameter (Fig. 8). These characteristics are briefly discussed in the following paragraphs.

A. Asymmetry

In the present study, asymmetry was analyzed by using novel method; Thresholding and Iterative Canny Method. This method cuts the image into two parts; an A image and an A' image, where A is the first cropped image and A' is the second cropped image, and, then, compares between them to identify differences and similarities with rotation in two-degree intervals from 0 to 360. After every two-degree increment rotation, the A and A' images are flipped from left to right. Afterwards, asymmetry is calculated for each image. For comparison of similarities, the Jaccard distance is calculated if there is similarity between the two pictures and the number of similarity times is counted (see Fig. 9):

$$Asymmetry = \frac{|A \cap A'|}{|A \cup A'|} = \frac{|A \cap A'|}{|A| + |A'| - |A \cap A'|}$$

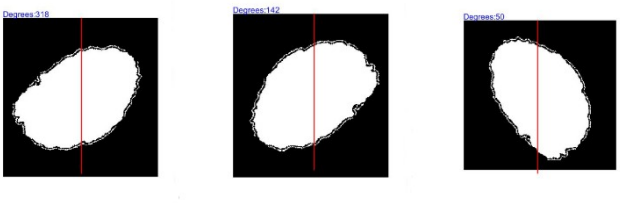

Fig. 9: Comparison of Similarities.

B. Border

Borders are drawn by using the Principal Component Analysis (PCA) and Iterative Canny Edge algorithms according to Otsu and novel method. This helps in delineating the shape of the border of spot for detection of irregular borders, if any. To this end, irregular points are calculated in the border after extracting the shape as shown in Fig. 10, which depicts the shape of a spot.

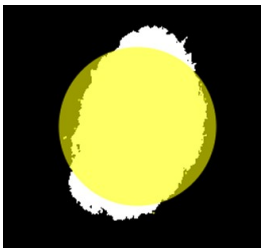

Fig. 10: Shape of a Spot.

In contrast to melanomas, a benign mole has smooth, even borders. Borders of early melanoma are usually uneven. There are several methods for calculating border irregularity, including the fractal index, compact index, pigment transition, and edge abruptness. In the current study, the researchers made use of 27 compact indices. The Density Index (DI) or Compact Index (CI) is extremely sensitive to the noise along edges. It may be computed using the following equation:

$$CI = \frac{P_L^2}{4\pi A_L}$$

where P and A are the perimeter and area of the lesion, respectively. Here, perimeter means the path surrounding an area. It is the length of the boundary of a closed figure.

C. Color

Number of the colors that are detected in a spot is calculated. The fixed colors of melanoma are black, white, red, light brown, dark brown, and light blue. Though, they can also be white, blue, or red.

Table 2 lists the six principal colors which appear in the malignant lesion and their corresponding RGB and Rgb values.

Table 2: The six principal colors which appear in the malignant lesion and their corresponding RGB and Rgb values.

Color	RGB	Rgb
White	255.255.255	1.0.1.0.1.0
Black	0.0.0	0.0.0.0.0.0
Red	255.0.0	1.0.0.0.0.0
Light-Brown	205.133.63	0.80.0.52.0.25
Dark-Brown	101.67.33	0.40.0.26.0.13
Blue-Gray	0.134.139	0.0.0.52.0.54

Color differences may be determined by computing the Euclidean distance between each two RGB pixels in the image according to the subsequent equation [28,29]:

$$D = \sqrt{(R_{rf} - R_{im})^2 + (G_{rf} - G_{im})^2 + (B_{rf} - B_{im})^2}$$

Eventually, the various colors in the image can be categorized into the six colors listed in Table 2 [28,29].

D. Diameter

Diameter of the spot is specified by halving the x and y values of the starting point from the center of the image toward the edges:

$$Diameter = \sqrt{\frac{4A}{\pi}}$$

8. GLCM Feature

The GLCM functions characterize the texture of an image by calculating how often pairs of pixels with particular values appear in a specified spatial relationship. To this end, energy, contrast, and 15 other features are extracted from the image. The mathematical formula and a description of each of those textural features are provided in Table 3.

9. Extraction of Features

In this step, all the features extracted using the ABCD rule and GLCM are compiled to compare them with the dataset using SVM and k-NN classifiers.

10. Classification Algorithms

In the present study, the researcher researched into computer algorithms for learning to do things like learning to automatically make an accurate prediction based on past observations (i.e., learning to complete a task; to make accurate predictions or behave intelligently). Machine learning focuses on automating methods. In other words, its goal is to create learning algorithms that learn automatically without the need for human intervention or assistance. Machine learning has several advantages, including that (i) it is, often, much more accurate than human-crafted rules because the machine learning systems are data-driven systems; (ii) it does not require a human expert or programmer; (iii) it automatically searches for hypotheses that can explain the patterns and trends in the data; (iv) it is inexpensive; and (iv) it can be applied to any learning task. On the other hand, it has some disadvantages such as the need for a large amount of labeled data and the inability to achieve perfect accuracy.

There are many different types of machine learning algorithms, one of which that we employed in the current study is the SVM algorithm. It is an algorithm that works to find a hyperplane in an N-dimensional space (N is the number of features) which distinctly classifies data points. The dataset of interest is trained and tested on classification. The features which were extracted from image are passed to SVM classifier so as to compare them with the training dataset for classification. Afterwards, the SVM training algorithm builds a model that maps new examples to one of a number of classes (two in the present study: benign tumor and malignant tumor). This makes the SVM classifier a non-probability binary linear classifier.

Neural Networks: This paper used the Back Propagation algorithm, which is supervised learning algorithm, for training multi-layer perceptron neural networks. Those networks initialize weights with random values because they do not know exactly what the weight can be. Therefore, they first give a small random weight if the model produces error with large values.

Evaluation of Machine Learning Classification

This paper compared the outputs of machine learning classifiers based on the effects of the uncertainty matrix so as to test the classification efficiency of the algorithms used. The quality metrics that were adopted in performance evaluation were the trustworthiness, sensitivity, accuracy, and precision. To compute values of these four metrics for the herein proposed lesion detection system, four statistical parameters were employed: false positive (FP), true positive (TP), true negative (TN), and false negative (FN). Definitions of these metrics are listed in Table 4.

Table 4: Performance Evaluation Terms.

Measure	Description
TP	Condition is correctly detected when present.
FP	Condition is not detected when absent.
FN	Condition is not detected despite being present.
TN	Condition is detected despite being absent.

Table 3: Textural Features of the GLCM.

Feature	Formula	Description
Auto-correlation	$\sum_{i=1}^{N_9}\sum_{j=1}^{N_9} ijp(i,j)$	Measure of the magnitude of fineness and coarseness of texture.
Contrast	$\sum_{i=1}^{N_9}\sum_{j=1}^{N_9}(i-j)^2 p(i,j)$	Measure of the local variations in the gray-level co-occurrence matrix.
Correlation	$\frac{\sum_{i=1}^{N_9}\sum_{j=1}^{N_9}(i-\mu)(j-\mu)p(i,j)}{\sigma^2}$	Measure of the joint probability occurrence of the specified pixel pairs.
Cluster Prominence	$\sum_{i=1}^{N_9}\sum_{j=1}^{N_9}((i-\mu)+(j-\mu))^4 p(i,j)$	Evaluates asymmetry of GLCM.
Cluster Shade	$\sum_{i=1}^{N_9}\sum_{j=1}^{N_9}((i-\mu)+(j-\mu))^3 p(i,j)$	Assesses the skewness of the GLCM matrix.
Dissimilarity	$\sum_{k=0}^{N_g-1} kp_{(x-y)}(k)$	Mean of gray level difference distribution.
Energy	$\sum_{i=1}^{N_9}\sum_{j=1}^{N_9} p(i,j)^2$	Measure of homogeneity of an image.
Entropy	$-\sum_{i=1}^{N_9}\sum_{j=1}^{N_9} p(i,j)\log_2(p(i,j))$	Measures randomness of image texture.
Homogeneity	$\sum_{i=0}^{N-1}\frac{p(i,j)}{1+(i-j)^2}$	Closeness of the distribution of elements in the GLCM to the diagonal.
Variance	$\sum_{i=0}^{N_g}\sum_{j=0}^{N_g}(i-\mu)^2 p(i,j)$	Assesses gray-level variability.

After defining the statistical indices consequently, the accuracy, sensitivity, specificity, and precision were computed as shown below.

$$Accuracy = \frac{(TP+TN)}{(TP+TN+FP+FN)}$$

$$Sensitivity = \frac{TP}{(TP+FN)}$$

$$Specificity = \frac{TN}{(TN+FP)}$$

$$Precision = \frac{TP}{(TP+FP)}$$

11. Classification

In this step, the outputs of feature extraction are input to SVM and other classifiers in order to determine the class to which the feature is closer.

12. Melanoma Detected

If the classification result is cancer, then the algorithm indicates the melanoma class, which is **Yes**.

13. Benign Detected

If the classification result is benign, then the algorithm points to the benign class, which is **No**.

14. Print Result

The classification result is then printed to the user as **Yes** if melanoma is detected and No if the detected lesion or tumor is benign.

5. Implementation

The cancer in the skin is examined and classified into stages using rules such as the ABCD Rule and GLCM texture metrics. Twenty-two features are used to classify the images with high accuracy. All of them must be taken into account in order to ensure accurate classification. Each button on the Graphical User Interface (GUI) executes distinct commands on the image and returns clear and highly accurate information to the user about what she/he is doing to facilitate smooth understanding of the process and its steps (Fig. 11). The different buttons on the GUI and their functions are described in the subsequent paragraphs.

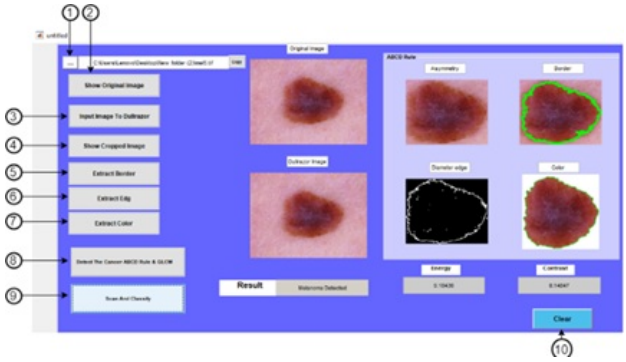

Fig. 11: The Graphical User Interface (GUI) of the Proposed System.

1. Pushbutton1 (Insert the Image)

This action introduces the image to be scanned to the system. The system opens the **Browse** tab (uigetfile) so that the user can select the image. When the user selects it, the system loads the image, saves its file path, and displays it in the bar (Testedit8).

2. Pushbutton2 (Show Original Image)

This action displays the selected image to the user. The system takes the image file path from **uigetfile** and saves it in the **OriginalImage** folder to display it to the user in the **axes1** window.

3. Pushbutton3 (Input Image to Dullrazor)
This action removes the hair from the image and filters it by using Dull-Razor software. The process involves three basic steps: spotting the locations of the dark hair; replacing the hair pixels with the nearby, non-hair pixels; and smoothing the image [25].

4. !dullrazor
The system opens the Dull-Razor software for the user by calling **!dullrazor**. In this step, the user should fill all fields with appropriate information, source file, and name and location of the target file, which must be named **skin** and have tif image format. This software takes the image, saves it into the **global image** folder, and presents it to the user in the **axes2** window as shown in Fig. 12.

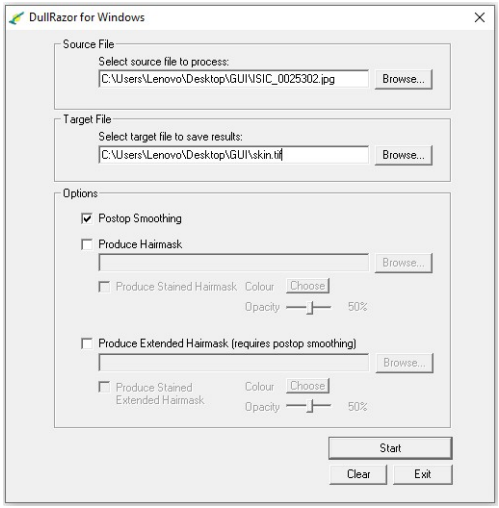

Fig. 12: DullRazor Software Interface.

Pushbutton4 (Show Cropped Image)
This step aims at cropping the suspect spots in the image using the asymmetry algorithm and showing it to the user. The system takes the image from the **global image** folder, sends it to the **Asymmetry** function, and returns the cropped image as shown in Fig. 13. Afterwards, it saves the cropped image into the **global RGB asymmetry** folder and presents it to the user in the **axes3** window.

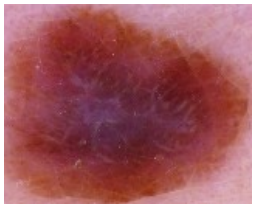

Fig. 13: Cropped image.

Pushbutton5 (Extract Border)
The objective of this function is to delineate the spot border using the Iterative Canny Edge method and show it to the user. The system takes the cropped image from the **global image** folder, draws the border of the spot in the image using the Canny edge function, determines the spot shape, and presents it to the user in the **axes4** window as illustrated in Fig. 14.

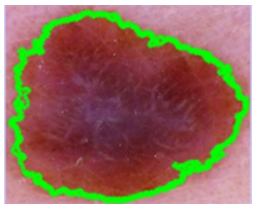

Fig. 14: Extracted Border.

Pushbutton6 (Extract Edge)
The goal of this function is to delineate the perimeter of the spot and present it to the user. Fig. 15 shows how the proposed system takes the image from the **global image** folder, calculates the diameter of the spot using the diameter function, and shows it to the user in the **axes5** window.

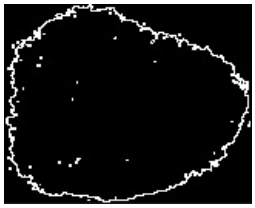

Fig. 15: Spot Perimeter.

Pushbutton7 (Extract Color)
This step aims at counting the colors selected from the image and displaying them to the user. The system takes the image from the **global image** folder, counts the colors

in it by using the color function, saves them in the **Finalscore** folder, and presents the produced image to the user. An example of how the extracted colors may look is given in Fig. 16.

Fig. 16: Extracted Colors.

Pushbutton8 (Detect the Cancer)
In this step, all the features in the image are processed using the ABCD Rule and GLCM for subsequent classification. The system takes the image from the **global image** folder, calls the GLCM function, and applies it to all the textural features in the image, saves those features in the **stats** folder, and displays them to the user as demonstrated in Fig. 17.

Fig. 17: Energy and the Contrast of the Image.

Pushbutton9 (Result)
The aim of this step is to provide the user with the final result of processing her/his image, whether the tumor, if any, is malignant or benign. As can be noticed in Fig. 18, the system takes the result of the execution of the ABCD Rule and the GLCM method (stats) and compares them with the dataset using the SVM classifier. After that, it saves them in the 'pred_final' folder and provides the user with the comparison outcomes.

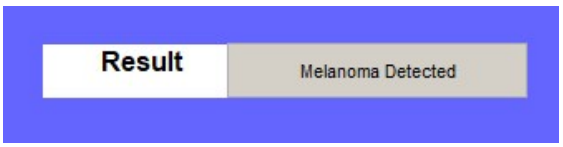

Fig. 18: Final Result.

Pushbutton10 (Clear)
The goal of this step is to remove all images and data from fields of the GUI in order to start over.

5 Result and discussion

This study employed SVM, NB, and k-NN classifiers and a dataset of dermoscopy images that comprised 4,000 images for training purposes and 1,500 images for testing. Almost 70%, 10%, and 20% of the images were allocated for training, validation, and testing, respectively. After the implementation of the code, it was observed that the results produced were highly close to the anticipated results. The values of the overall classification error associated with the SVM, k-NN, and NB classifiers were 5.65%, 14.50%, and 21.00%, respectively. The values of the classification accuracy of the SVM, k-NN, and NB classifiers were 94.35%, 85.50%, and 78.95%, respectively. As Tables 5 to 10 demonstrate, the classification error and accuracy values provide evidence that the SVM classifier performs better than both the NB and k-NN classifiers.

Table 5: Results of SVM Training

Classification Matrix			
Benign	**1924** 48.00%	**121** 3.00%	**94%** 5.9%
Melanoma	**73** 1.80%	**1882** 47.20%	**96.3%** 3.7%
Overall	**96.4%** 3.60%	**93.9%** 6.10%	**95.15%** 4.80%

Table 6: Results of SVM Testing

Classification Matrix			
Benign	**752** 50.13%	**49** 3.26%	**93.9%** 6.10%
Melanoma	**36** 2.40%	**663** 44.2%	**94.8%** 5.20%
Overall Accuracy	**95.4%** 4.56%	**93.1%** 6.88%	**94.35%** 5.65%

Classification performance is crucial for the successful detection and sound diagnosis of skin cancer lesions. Hence, the particular features to extract and the classifier to employ ought to be carefully selected. This paper introduces an automated system for detection and diagnosis of skin cancer lesions that has the ability to extract differing features from dermoscopy images. The system proposed here employed the NB, k-NN, and SVM classifiers, which are the three most common classification algorithms. The processes involved were

Table 7: Results of k-NN Classifier Training

Classification Matrix			
Benign	**1763** 44.10%	**216** 5.40%	**89.1%** 10.90%
Melanoma	**292** 7.30%	**1729** 43.20%	**85.6%** 14.40%
Overall Accuracy	**85.8%** 14.20%	**88.9%** 11.10%	**87.35%** 12.60%

Table 8: Results of k-NN Classifier Testing

Classification Matrix			
Benign	**673** 44.90%	**128** 8.53%	**84%** 16.00%
Melanoma	**91** 6.00%	**608** 40.50%	**87%** 13.00%
Overall Accuracy	**88%** 12.00%	**83%** 17.00%	**85.5%** 14.50%

Table 9: Results of Training of the NB Classifier

Classification Matrix			
Benign	**1660** 41.50%	**319** 8.00%	**84%** 16.00%
Melanoma	**401** 10.00%	**1620** 40.50%	**80%** 20.00%
Overall Accuracy	**80.5%** 19.50%	**83.5%** 16.50%	**82%** 18.00%

Table 10: Results of Testing of the NB Classifier

Classification Matrix			
Benign	**619** 41.20%	**182** 12.10%	**77.27%** 22.70%
Melanoma	**135** 9.00%	**564** 37.60%	**80.7%** 19.30%
Overall Accuracy	**82.1%** 17.90%	**75.6%** 24.40%	**78.95%** 21.00%

image pre-processing and segmentation using thresholding, filtering, and statistical feature extraction using the GLCM and ABCD algorithms. This study employed a dataset of dermoscopy images consisting of 5,500 images. It then employed k-NN, SVM, and NB classifiers in order to classify the dermoscopy images into two groups based on the condition of the skin: melanoma and benign skin. Afterwards, a comparison was held between the extracted features and the features of dermoscopy images in the dataset. Values of classification accuracy of these classifiers in the testing phase are provided by the classification matrix (Tables 8, 9, and 10).

6 Conclusions

The results of assessment of performance of the system proposed in this paper revealed that the overall classification accuracy and classification error of the SVM classifier in the training phase were 95.15% and 4.8%, respectively (Table 11). The corresponding values during the testing phase were 94.35% and 5.65%, respectively. As to the k-NN classifier, the classification accuracy and error in the training phase were 87.53% and 12.65%, respectively. During the testing phase, however, the classification accuracy and error of this classifier were 85.5% and 14.4%, respectively. In the case of the NB classifier, the overall classification accuracy and error during the training phase were 82% and 18%, respectively. Meanwhile, the overall classification accuracy and error of the NB classifier during the testing phase were 78.95% and 21%, respectively. The values of the classification performance metrics (accuracy, precision, sensitivity, and specificity) of the three classifiers employed in this study are given in Table 11.

Table 11: Values of Classification Performance Metrics of the Three Classifiers

Classifier	Accuracy	Precision	Sensitivity	Specificity
SVM	94.35%	96.3%	93.1%	95.4%
k-NN	85.5%	85.6%	83.0%	88.0%
NB	78.95%	80.7%	75.6%	82.1%

Acknowledgment

I would like to acknowledge the initial support received from Jadara University under grant number Jadara-SR-Full2023. This support played a vital role in facilitating this research. The author would like to thank the editor and anonymous reviewers for their comments that help improve the quality of this work.

Ethics

This manuscript is original work and has not been submitted for publication elsewhere. The corresponding Author ensures that his colleague have read and approved the manuscript and no ethical issues involved.

References

[1] Siegel RL, Miller KD, Wagle NS, Jemal A. Cancer statistics, 2023. **CA Cancer J Clin 73**(1), 17–48. https://doi.org/10.3322/caac.21763

[2] Michelini S, et al. Combining reflectance confocal microscopy, optical coherence tomography and ex-vivo fluorescence confocal microscopy for margin assessment in basal cell carcinoma excision. **Dermatol Pract Concept 14**(2), e2024090. https://doi.org/10.5826/dpc.1402a90

[3] Mahmoud Abdel-salam, Saleh Ali Alomari, Mohammad H. Almomani, et al. Quadruple strategy-driven hiking optimization algorithm for low and high-dimensional feature selection and real-world skin cancer classification. **Knowl Based Syst 315**, 113286. https://doi.org/10.1016/j.knosys.2025.113286
[4] Forde PM, Spicer J, Lu S, et al. Neoadjuvant nivolumab plus chemotherapy in resectable lung cancer. **N Engl J Med 386**(21), 1973–1985. https://doi.org/10.1056/NEJMoa2202170
[5] Mothoneos J. Designer: Pelosi E. Printer: SOS Print + Media Group. Understanding Skin Cancer. Published March 2012, This edition January 2018, 6–12, 31. ISBN 9781925136180.
[6] Yang G, Luo S, Greer P. Advancements in skin cancer classification: a review of machine learning techniques in clinical image analysis. **Multimed Tools Appl**. https://doi.org/10.1007/s11042-024-19298-2
[7] Siegel RL, Giaquinto AN, Jemal A. Cancer statistics, 2024. **CA Cancer J Clin 74**(1). https://doi.org/10.3322/caac.21820
[8] Lembhe A, Motarwar P, Patil R, Elias S. Enhancement in skin cancer detection using image super resolution and convolutional neural network. **Procedia Comput Sci 218**, 164–173. https://doi.org/10.1016/j.procs.2022.12.412
[9] Dascalu A, David EO. Skin cancer detection by deep learning and sound analysis algorithms: a prospective clinical study of an elementary dermoscope. **EBioMedicine 43**, 107–113. https://doi.org/10.1016/j.ebiom.2019.04.055
[10] Sol S, Boncimino F, Todorova K, Waszyn SE, Mandinova A. Therapeutic approaches for non-melanoma skin cancer: standard of care and emerging modalities. **Int J Mol Sci 25**(13), 7056. https://doi.org/10.3390/ijms25137056
[11] Dixon AJ, Sladden M, Zouboulis CC, Popescu CM, Nirenberg A, Steinman HK, Longo C, Dixon ZL, Thomas JM. Primary cutaneous melanoma—management in 2024. **J Clin Med 13**(6), 1607. https://doi.org/10.3390/jcm13061607
[12] Corchete-Snchez L, Corchado-Cobos R, Garca-Sancha N, Cardona-Machado C, Baeza-Hernndez G, Prez-Losada J, Caueto J. Identification of two transcriptomic subgroups in actinic keratosis: differentiation between normal skin and cutaneous squamous cell carcinoma-like profiles using RNA-seq. **EJC Skin Cancer 2**(Suppl 1), 100032. https://doi.org/10.1016/j.ejcskn.2024.100032
[13] Cives M, Mannavola F, Lospalluti L, Sergi MC, Cazzato G, Filoni E, Cavallo F, Giudice G, Stucci LS, Porta C, et al. Non-melanoma skin cancers: biological and clinical features. **Int J Mol Sci 21**(15), 5394. https://doi.org/10.3390/ijms21155394
[14] Alquran H, et al. The melanoma skin cancer detection and classification using support vector machine. In: **2017 IEEE Jordan Conference on Applied Electrical Engineering and Computing Technologies (AEECT)**, 1–6. https://doi.org/10.1109/AEECT.2017.8257738
[15] Nasr I, McGrath EJ, Harwood CA, et al. British Association of Dermatologists guidelines for the management of adults with basal cell carcinoma 2021. **Br J Dermatol 185**(5), 899–920. https://doi.org/10.1111/bjd.20524
[16] Bano U, Sarode T. Skin Cancer Detection Using Image Processing. **Int J Innov Res Sci Eng Technol 4**(4), 2875–2880.
[17] Smaoui N, Bessassi S. A developed system for melanoma diagnosis. **Int J Comput Vis Signal Process 3**(1), 10–17.
[18] Jana E, Subban R, Saraswathi S. Research on Skin Cancer Cell Detection using Image Processing. **Proc IEEE Int Conf Comput Intell Comput Res**, 1–7.
[19] Christensen SR, Wilson LD, Leffell DJ. Chapter 90: Cancer of the Skin. In: **American Cancer Society. Facts & Figures 2019**. American Cancer Society, Atlanta, GA, 1–5.
[20] Iyatomi H, et al. Quantitative assessment of tumour extraction from dermoscopy images and evaluation of computer-based extraction methods for an automatic melanoma diagnostic system. **Melanoma Res 16**(2), 183–190. https://doi.org/10.1097/01.cmr.0000215041.76553.58
[21] Vijayalakshmi MM. Melanoma skin cancer detection using image processing and machine learning. **Int J Trend Sci Res Dev 3**(4). https://doi.org/10.31142/ijtsrd23936
[22] Viknesh, Kaushik C, Kumar PN, Seetharaman R, Anitha D. Detection and classification of melanoma skin cancer using image processing technique. **Diagnostics 13**(21), 3313. https://doi.org/10.3390/diagnostics13213313
[23] Mahmoud NM, Soliman AM. Early automated detection system for skin cancer diagnosis using artificial intelligent techniques. **Sci Rep 14**, 9749. https://doi.org/10.1038/s41598-024-59783-0
[24] Kandhro IA, et al. Performance evaluation of E-VGG19 model: enhancing real-time skin cancer detection and classification. **Heliyon 10**(10), e31488. https://doi.org/10.1016/j.heliyon.2024.e31488
[25] Farooq MA, Azhar MAM, Raza RH. Automatic lesion detection system (ALDS) for skin cancer classification using SVM and neural classifiers. In: **2016 IEEE 16th International Conference on Bioinformatics and Bioengineering (BIBE)**, 301–306. https://doi.org/10.1109/BIBE.2016.53
[26] ISIC Archive. https://www.isicarchive.com/#!/topWithHeader/wideContentTop/main (accessed Jan. 09, 2025).
[27] Russel S, Norvig P. Artificial intelligence—a modern approach, 3rd Edition. **Knowl Eng Rev**. https://doi.org/10.1017/S0269888900007724
[28] Jain AK. Fundamentals of digital image processing. Prentice Hall, 569.
[29] Sezgin, M., Sankur, B., 2004. Survey over image thresholding techniques and quantitative performance evaluation. *Journal of Electronic Imaging* 13(1), 146?165. Available at: https://doi.org/10.1117/1.1631315.
[30] Tomatis S, et al. Automated melanoma detection: multispectral imaging and neural network approach for classification. **Med Phys 30**(2), 212–221. https://doi.org/10.1118/1.1538230
[31] Priyanka, Kumar D. Feature extraction and selection of kidney ultrasound images using GLCM and PCA. **Procedia Comput Sci 167**, 1722–1731. https://doi.org/10.1016/j.procs.2020.03.382
[32] Upadhyay M, Kriti, Rawat J. A review of recent machine learning techniques used for skin lesion image classification. In: **Advancements in Bio-Medical Image Processing and Authentication in Telemedicine**, 76–90. https://doi.org/10.4018/978-1-6684-6957-6.ch005
[33] Al-Batah M, Zaqaibeh B, Alomari SA, Alzboon MS. Gene microarray cancer classification using correlation

based feature selection algorithm and rules classifiers. **Int J Online Biomed Eng 15**(8). https://doi.org/10.3991/ijoe.v15i08.10617

[34] Abualigah L, Al-Okbi NK, Alomari SA, et al. Optimized image segmentation using an improved reptile search algorithm with Gbest operator for multi-level thresholding. **Sci Rep 15**, 12713. https://doi.org/10.1038/s41598-025-96429-1

Saleh Ali K. Alomari obtained his MSc and PhD in Computer Science from Universiti Sains Malaysia (USM), Pulau Penang, Malaysia in 2008 and 2013 respectively. He is a lecturer at the faculty of Information Technology, Jadara University, Irbid, Jordan. He is Assistance Professor at Jadara University, Irbid, Jordan 2013. He is a head of the computer network department at Jadara University, 2014 until 2016. He is the candidate of the Multimedia Computing Research Group, School of Computer Science, USM. He is research assistant with Prof. Dr. Putra, Sumari. He is managing director of ICT Technology and Research and Development Division (R&D) in D&D Professional Consulting Company. He has published over 50 papers in international journals and refereed conferences at the same research area. He is a member and reviewer of several international journals and conferences (IEICE, ACM, KSII, JDCTA, IEEE, IACSIT, etc). His research interest are in area of multimedia networking, video communications system design, multimedia communication specifically on Video on Demand system, P2P Media Streaming, MANETs, caching techniques and for advanced mobile broadcasting networks as well.